Simulations of dynamos in compressible flows

Lecture 2: Galactic applications

Maarit J. Korpi

maarit.korpi@helsinki.fi

Division of Geosciences and Astronomy

Department of Physics

University of Helsinki

Lecture 2: Galactic applications

- Sources of interstellar turbulence
- Thermal instability and regulation of the warm and cold phases
- Multiphase picture of the ISM
- Supernova explosions
- Magnetorotationally-driven dynamos
- Implications for galactic dynamo

Sources of interstellar turbulence

- Various sources of turbulence
  - Differential rotation
  - Magnetorotational instability (MRI)
  - Parker instability
  - Stellar forcing (winds, radiation pressure, SNe)
  - Thermal instability
  - Gravitational instability ...
- Energetically SNe dominate in the star-forming disk
- In the outer regions MRI and other instabilities?
- Different dynamo regimes?

Thermal instability (1)

The existence of the hot component of the interstellar medium was discovered in the 1970s. Before that time, the ISM was thought to consist of cold molecular clouds surrounded with warmer diffuse medium. Field, Goldsmith and Habing (1969) showed that such a two-phase medium can be spontaneously formed in a medium where a thermally unstable phase (G) exists between two thermally stable phases (F and H). Let us define a net function for heating (Γ) and cooling (Λ) processes as

$$\mathcal{L} \equiv \rho\Lambda - \Gamma,$$

indicating net heating when $\mathcal{L} < 0$ and net cooling when $\mathcal{L} > 0$. Condition for thermal instability reads

$$\left(\frac{\partial \mathcal{L}}{\partial T}\right)_A < 0 \ \ \text{(unstable)},$$

where A stands for one of the thermodynamic variables ρ, p, s.

$$\begin{aligned}
\left(\frac{\partial \mathcal{L}}{\partial T}\right)_\rho &< 0, \ \text{(ISOCHORIC)} \\
\left(\frac{\partial \mathcal{L}}{\partial T}\right)_p = \left(\frac{\partial \mathcal{L}}{\partial T}\right)_\rho - \frac{\rho_0}{T_0}\left(\frac{\partial \mathcal{L}}{\partial \rho}\right)_T &< 0, \ \text{(ISOBARIC)} \\
\left(\frac{\partial \mathcal{L}}{\partial T}\right)_s = \left(\frac{\partial \mathcal{L}}{\partial T}\right)_\rho + \frac{1}{\gamma - 1}\frac{\rho_0}{T_0}\left(\frac{\partial \mathcal{L}}{\partial \rho}\right)_T &< 0, \ \text{(ISENTROPIC)}
\end{aligned}$$

Thermal instability (2)

The above stability criteria can be derived analytically by linear stability analysis, originally presented by Field (1965). The isobaric mode is the most important one in the ISM, also called as the condensation mode, and the corresponding stability criterion as the Field criterion. The two-phase model of FGH can be understood with the Field stability criterion and the graph below.

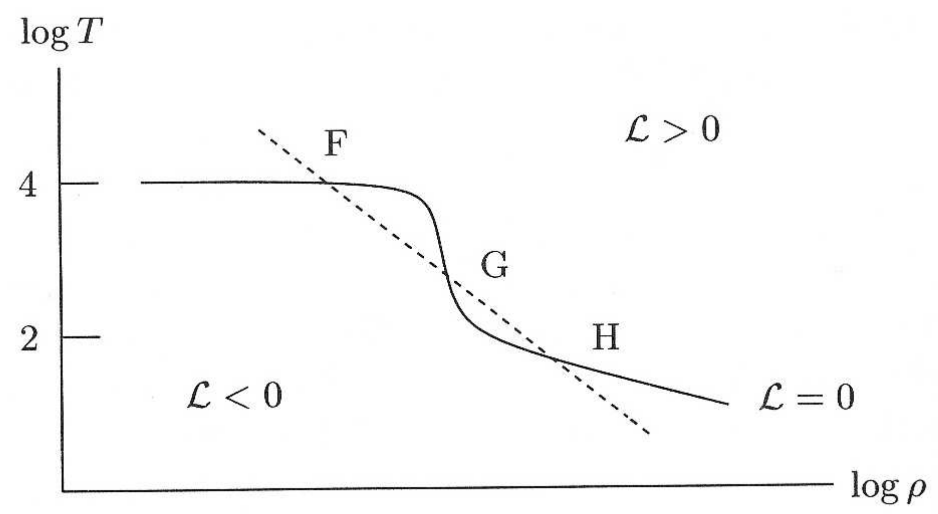

Thermal instability (3)

TI seems not to be capable of driving self-sustained turbulence (Brandenburg, Korpi & Mee 2007), and therefore is not a process solely responsible for dynamo action.

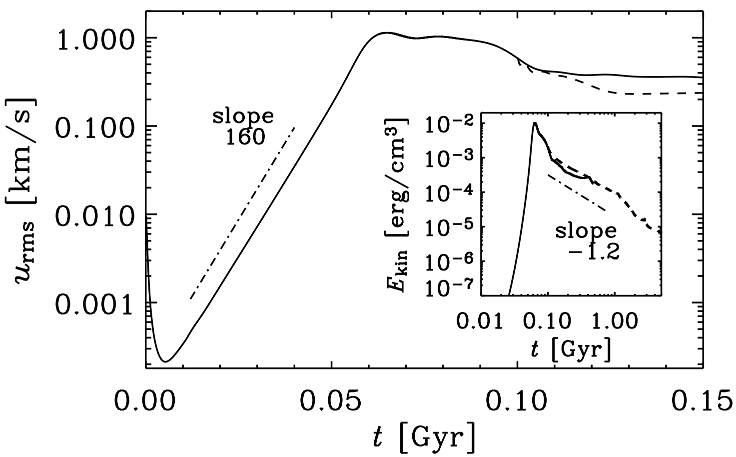

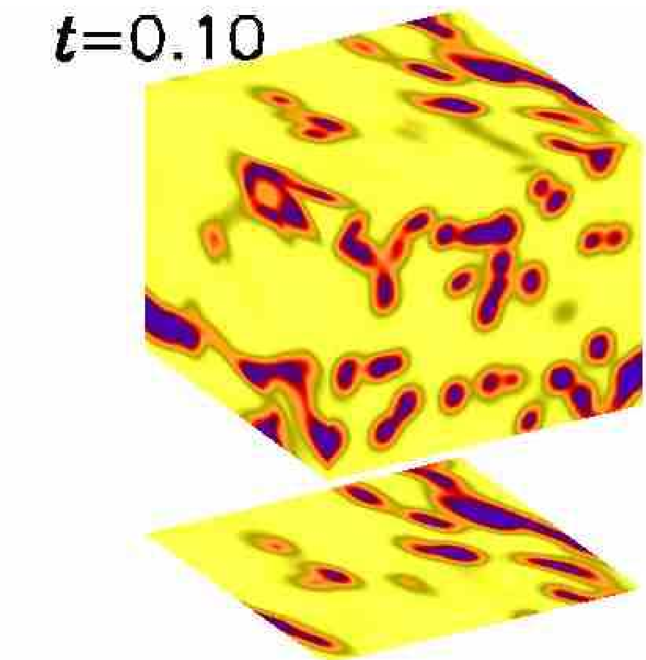

Example with the PENCIL CODE

TI can, however, significantly affect dynamo action. Here two forced turbulence runs (helical turbulence) in a cubic domain, differing by the cooling function, are compared. The black line represents a run with thermally stable cooling function $\Lambda = C_i T^{\beta_i}$, for which all $\beta_i > 1$. The orange line shows a run with thermally unstable cooling function, for which $\beta = 0.56$ between the temperature range of 313 and 6102 K. The coefficients C_i of the cooling functions have been scaled so that $\mathcal{L}$ is approximately the same.

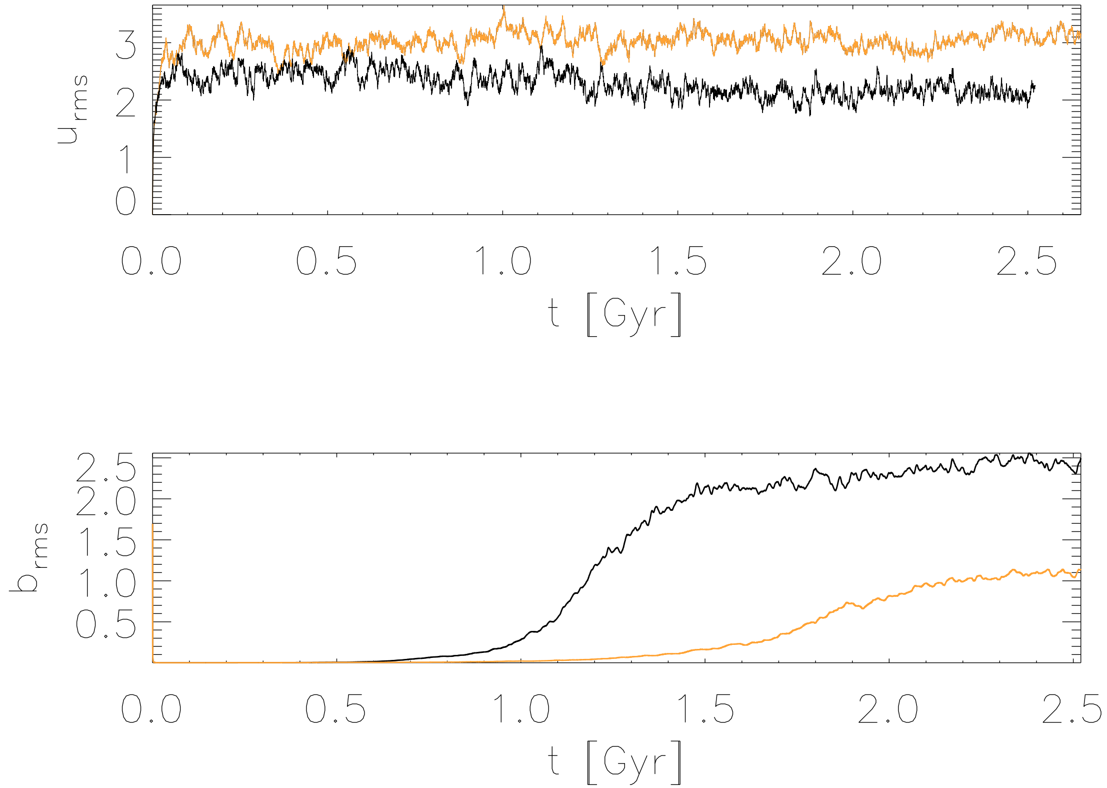

Example with the PENCIL CODE

Thermally unstable flow has significantly more kinetic energy, while the growthrate and saturation level of the magnetic field is significantly lower in the unstable case. Also the flow structures are very different; thermally stable cooling function exhibits stronger density-magnetic field correlation, while in the thermally unstable flow these two quantities are not clearly correlated. [*Homework for Anvar: pls write up the draft!*]

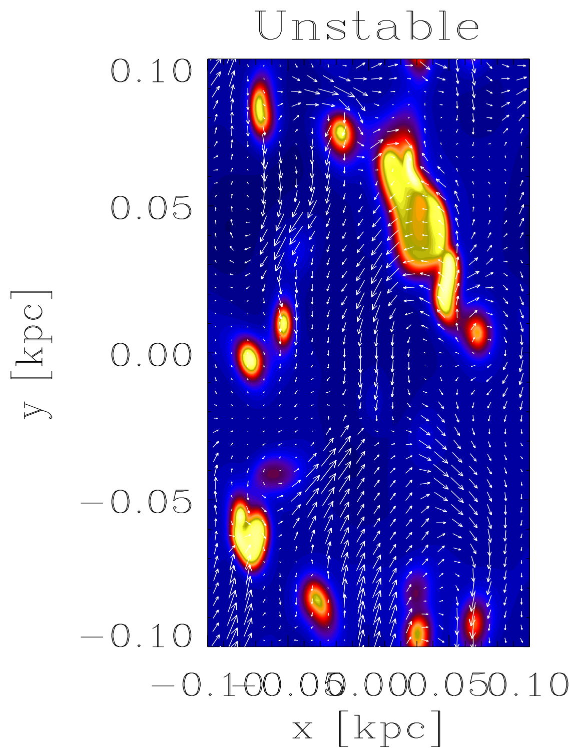

Supernovae (1)

- Massive stars end their lives exploding as SNe
- In a SN, roughly 10^{51}ergs of energy is released
- Energy goes into heating, compressing and accelerating the ISM, some of it gets radiated away
- Formation of a spherical shock in a quiescent environment
- More complex structure in a nonuniform environment
- Turbulent state results from the interaction of new and old SNe
- SNe create and maintain a hot phase in the ISM, discovered observationally in the 1970's.

Multiphase picture

- Three main phases: cold, warm and hot
- No discrete equilibrium states, rather a continuum
- Rough pressure equilibrium, but pressure distribution has wide wings (as can be seen, e.g. in the models of Korpi et al. 1999)

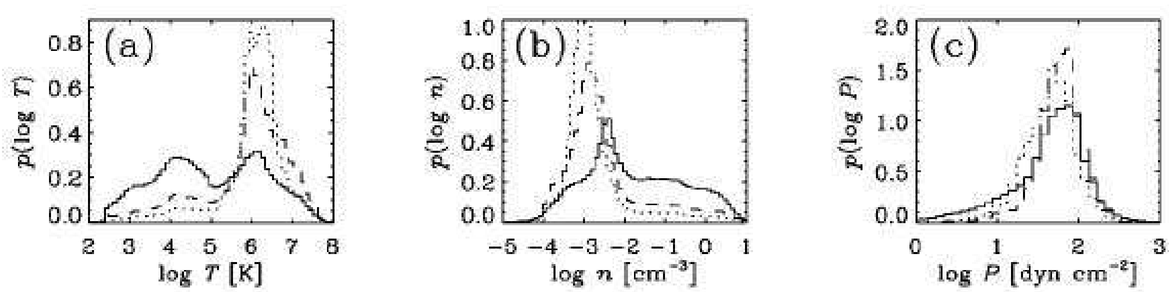

Supernovae (2)

The first theories that could be applied to the evolution of supernova remnants came from atomic–weapon research, when Sedov (e.g. Sedov 1959) and Taylor (1950) independently developed a theory for strong point–like explosions in a uniform quiescent medium. This theory is based on dimensional arguments and self-similarity of the generated shock wave.

In the following we assume that the ambient pressure p_0 is small compared to the pressure inside the remnant and therefore can be neglected. Let us also neglect magnetic fields and radiative losses (adiabatic case). It sounds reasonable to assume, that the radius of the expanding remnant would depend on time, the ambient density ρ_0, and on the energy of the explosion E_0, i.e.

$$R(t) = \alpha E_0^a \rho_0^b t^c,$$

where α is a dimensionless quantity. Let us now write the units of energy and density with the help of the basic units $[R]$ and $[t]$: $[E_0] = [m][R]^2[t]^{-2}$ ja $[\rho_0] = [m][R]^{-3}$. Requiring that the left and right hand sides have the same units we obtain

$$[R] = \left(\frac{[m][R]^2}{[t]^2}\right)^a \left(\frac{[m]}{[R]^3}\right)^b [t]^c$$

Supernovae (3)

From here we get a set of equations

$$
\begin{aligned}
[t] \rightarrow 0 &= -2a + c \\
[R] \rightarrow 1 &= 2a - 3b \\
[m] \rightarrow 0 &= a + b,
\end{aligned}
$$

wherefrom $a = 1/5$, $b = -1/5$ and $c = 2/5$, yielding

$$R(t) = \alpha \left(\frac{E_0 t^2}{\rho_0} \right)^{1/5} .$$

Differentiating this for time gives the velocity

$$U(t) = \frac{dR}{dt} = \frac{2}{5} \alpha \left(\frac{E_0}{\rho_0 t^3} \right)^{1/5} .$$

At the shock front the Rankine–Hugoniot jump conditions (derived earlier) hold. Since the flow is self–similar, the shapes of distributions for density, pressure and velocity do not change in time, in other words the solutions can be expressed as

$$\rho = \rho_s \rho^*(\alpha),\ p = p_s(t) p^*(\alpha) \text{ and } u = u_s(t) u^*(\alpha),$$

where $\rho^*,\ p^* \text{ and } u^*$ are dimensionless functions.

Supernovae (4)

The Sedov–Taylor solution can be obtained by substituting these expressions into the fluid equations for the spherically symmetric and adiabatic case, and solving for the dimensionless functions. Sedov (1959) succeeded in finding an exact analytical solution using a technique employing the energy integral, whereas Taylor integrated the equations numerically. The α-parameter turned out to be approximately 1.17 from their analyses. Figure: Solid line, 1D-case; dotted line, 2D-case; dashed line, 3D-case.

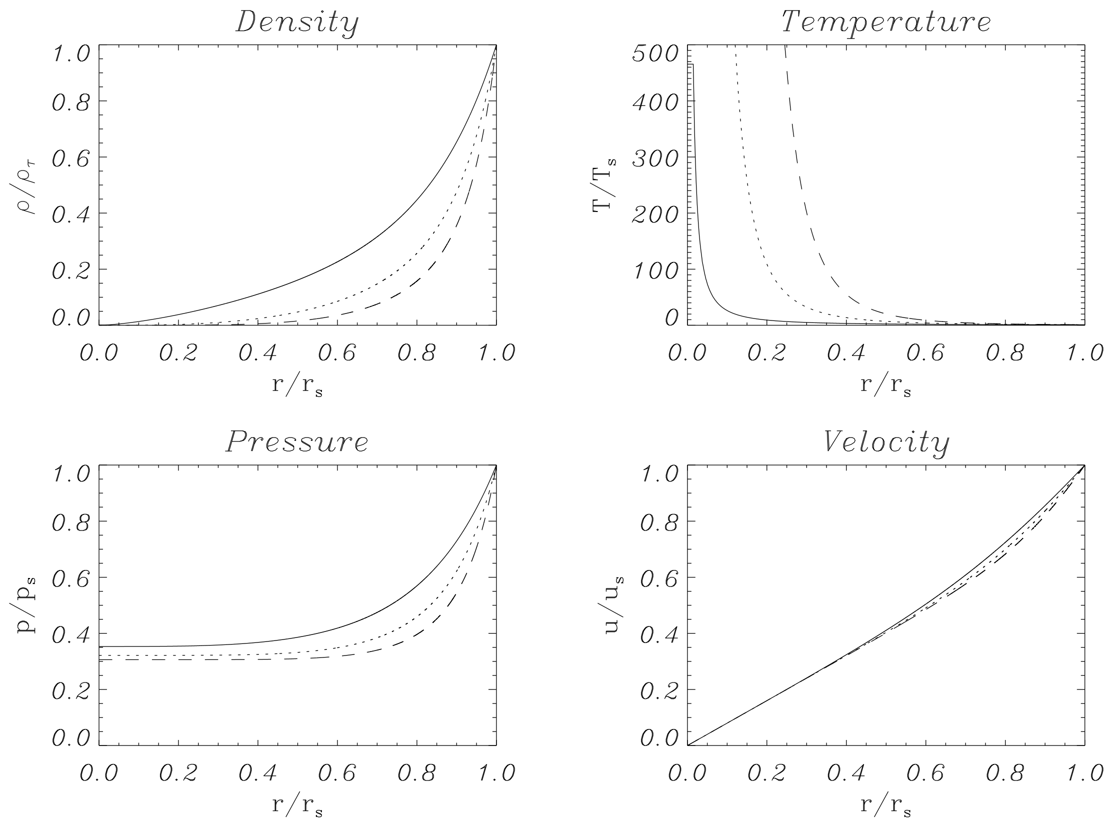

Example with the PENCIL CODE

Numerical models trying to simulate a SN can be tested against the Sedov–Taylor expansion law and/or full solution. Using upwinding differences for all variables plus shock viscosity of $\nu_{\rm shk}$=2 produces quite satisfactorily the Sedov solution (expected radius and density contrast marked with a star) with the PENCIL CODE.

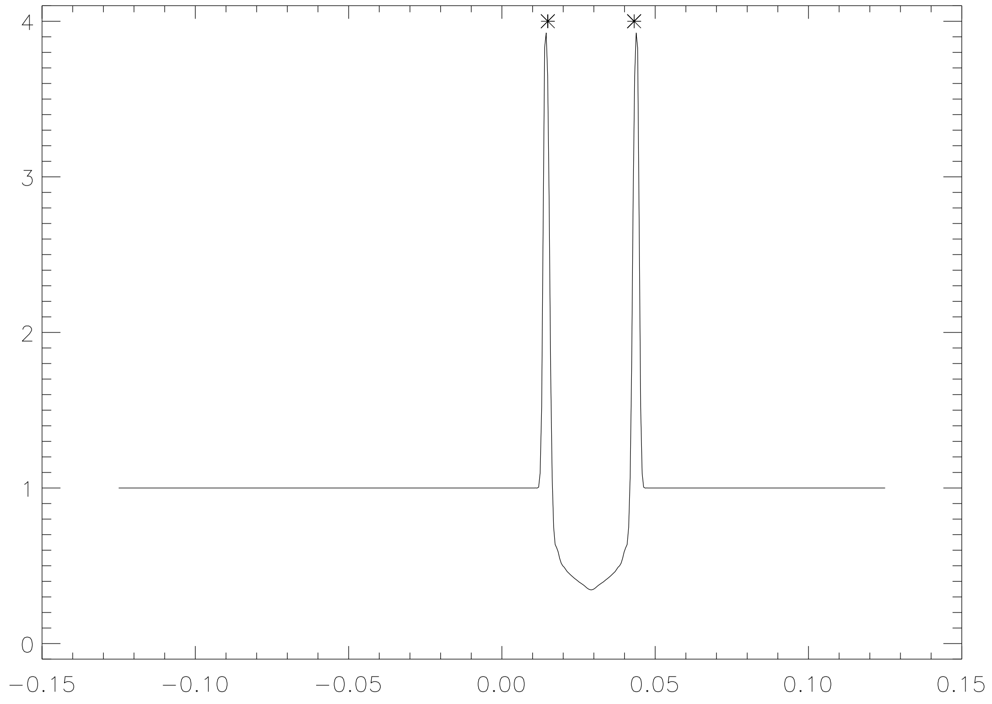

Supernovae and vorticity

Supernova forcing is of potential (or irrotational) type, i.e. the flow resulting from a single spherical shock in uniform, stationary medium or several non-interacting shocks under the same conditions, possesses no vorticity, i.e.

$$\omega = \nabla \times \boldsymbol{u} = 0.$$

The vorticity equation can be obtained from the velocity equation by taking a curl

$$\frac{D\boldsymbol{\omega}}{Dt} = (\boldsymbol{\omega} \cdot \nabla)\, \boldsymbol{u} - \boldsymbol{\omega}\, (\nabla \cdot \boldsymbol{u}) + \frac{1}{\rho^2} \nabla \rho \times \nabla p + \text{viscous terms.}$$

The first two terms in the RHS describe vortex stretching due to velocity gradients and compressibility, and the third one is the baroclinic term, which can also be expressed as $\nabla T \times \nabla s$. Vorticity can also be generated due to viscous effects, but this can be assumed to take place at the small scales. For barotropic flows, the baroclinic term vanishes. For two-dimensional flows, the vortex stretching term vanishes. In three dimensions, however, small amounts of vorticity generated can be exponentially amplified by the vorte stretching term.

Supernovae and vorticity

Korpi et al. (1999) investigated vorticity generation in density stratified, rotating and shearing SN forced flows. On the left we show the time evolution of the baroclinic term contribution (dashed) and vortex stretching term contribution (solid) to the time evolution of vorticity. On the right hand side we show the angle between ∇T and ∇s near the midplane (upper curves) and overe the whole computational volume (lower curves). It is evident that significant amounts of vorticity is generated at earlier times by the baroclinic term in the regions of higher SN density. At later times, the vortex stretching term effectively amplifies the vorticity. Due to the effective generation of vorticity, SN flows are largely helical.

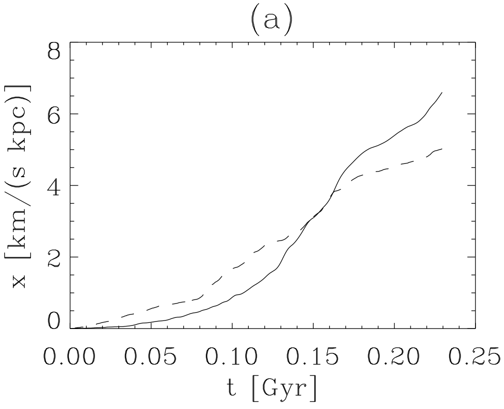

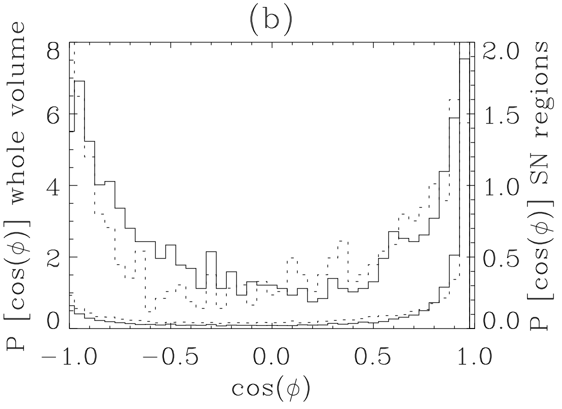

Supernovae and dynamos

In the calculations of Korpi et al. (1999) rotation rate and profile, and the SN frequency of the Milky Way at the solar neighorhood was used, i.e. $\Omega_0 = 25$kms^{-1}kpc^{-1}, the rotation curve was assumed to be flat with $\Omega \propto R^{-q},\ q = 1$, SNe frequencies $f_{\rm SNII} = 1/44$yr^{-1} and $f_{\rm SNI} = 1/330$yr^{-1}. Type I SNe were distributed randomly in the horisontal plane, whereas type II SNe were correlated in space. The vertical distribution was exponential, with scaleheights $h_{\rm SNII} = 90$pc and $h_{\rm SNI} = 325$pc. Thermally *stable* cooling function was used. No dynamo action was observed.

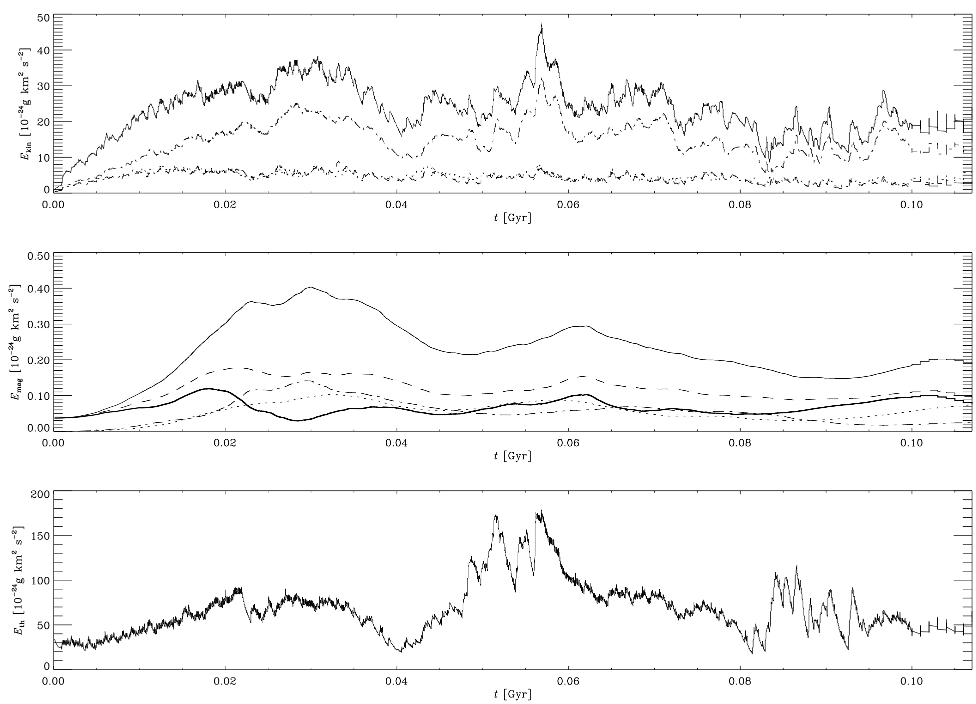

Supernovae and dynamos

Although no exponential growth of the magnetic field could be seen, we observed the generation of a mean radial field B_x and a mean azimuthal field B_y. Since the vertical flux vanishes ($B_z = 0$) due to the periodic boundaries used in radial and azimuthal directions, B_x can be regenerated from B_y if there is a z–dependent azimuthal mean electromotive force. In the case of an $\alpha\Omega$–dynamo, a linear correlation

$$\mathcal{E}_y = \alpha B_y$$

would exist. Then the weak radial field could be sheared out to produce the stronger mean azimuthal field. On the left panel we plot the mean azimuthal magnetic field against the mean azimuthal electromotive force calculated for the upper disk plane, the averages calculated over a timespan of 10 Myrs. The right panel shows the same for the lower disk plane. There is a rather tight linear correlation, with $\alpha \pm 6$ km s^{-1}, the minus sign corresponding to the lower and the plus sign to the upper part of the disk (Korpi 1999, PhD thesis).

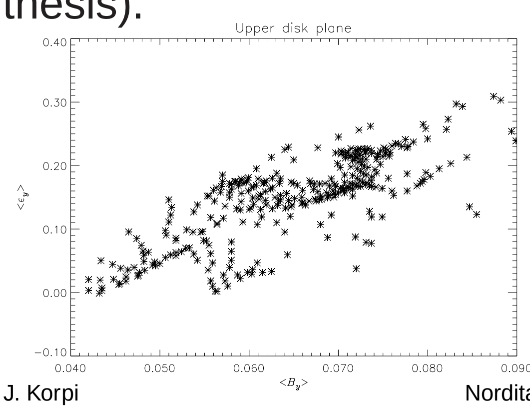

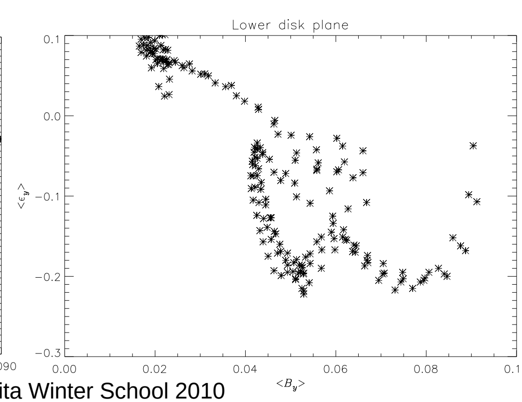

Supernovae and dynamos

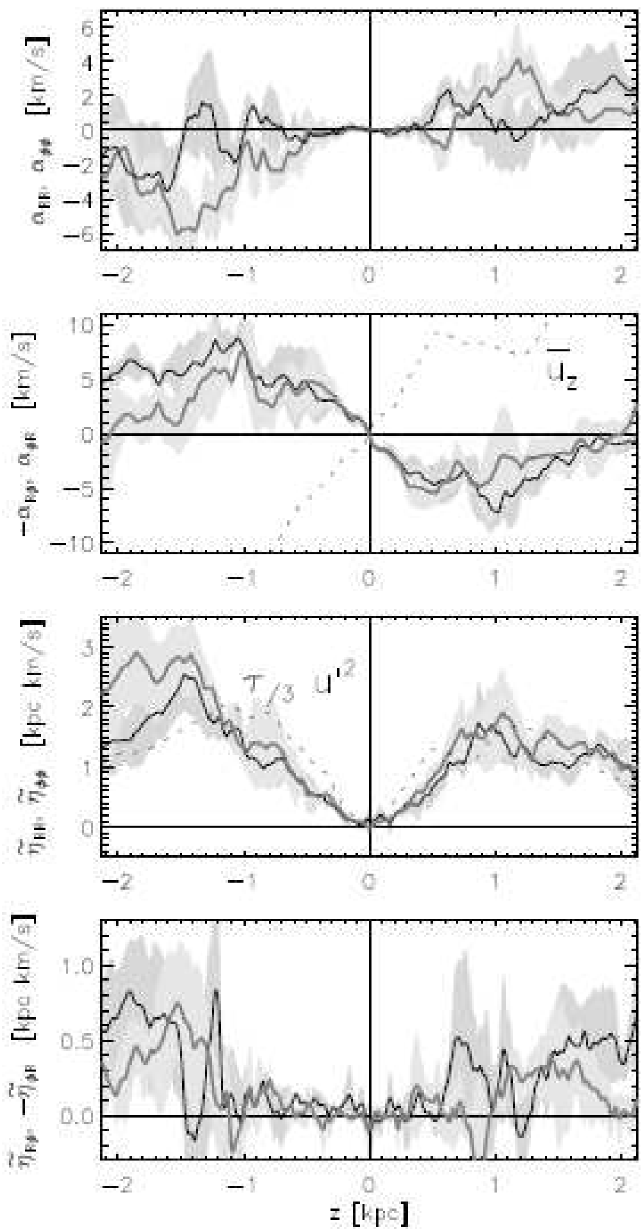

Gressel et al. (2008) made similar simulations with the NIRVANA code, the main difference being the usage of thermally *unstable* cooling function for certain T range. For the rotation rate of the Milky Way, no dynamo action was seen. For four times higher rotation rate, dynamo action was seen. The test field method was used, and the mean-field transport coefficients derived, the figure shows the results of a run with half the galactic SN frequency but four times the rotation rate.

Magnetorotational instability

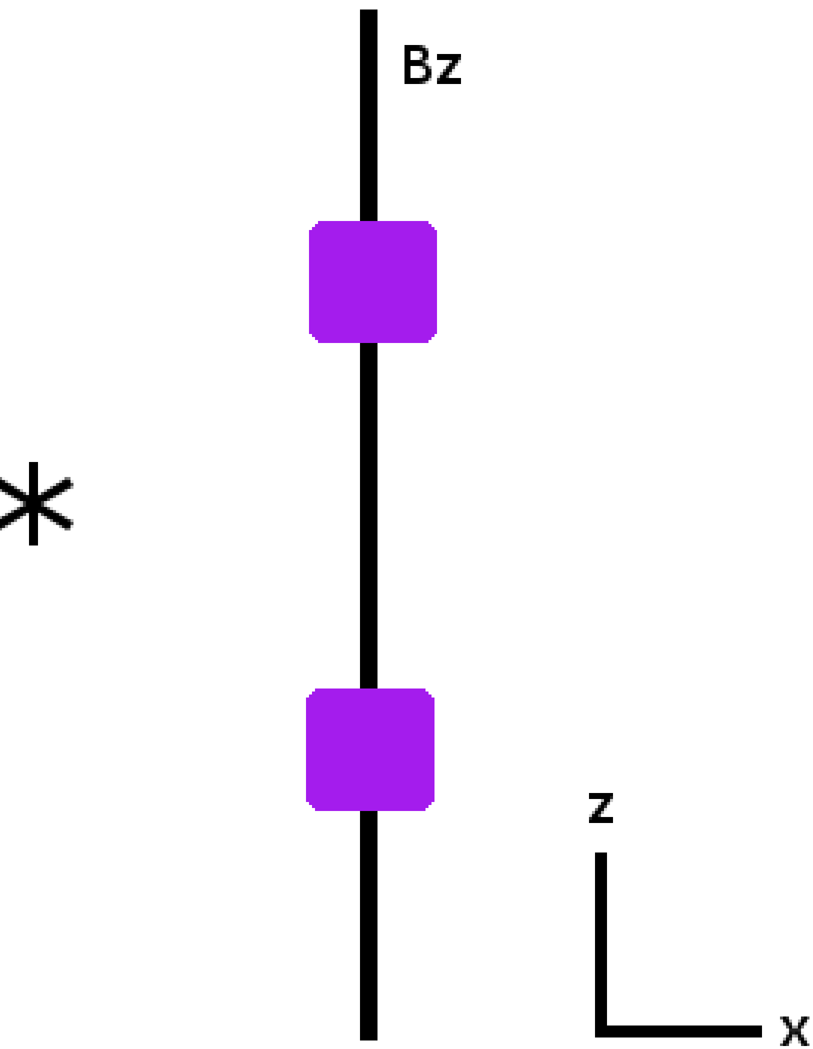

Differentially rotating flows can be destabilised by the presence of a weak ($\beta = \frac{p_{\rm ther}}{p_{\rm mag}} > 1$) magnetic field, if the rotation law is such that

$$\frac{d\Omega^2}{dR} < 0,$$

translating into $q > 0$ for rotation laws of the type $\Omega \propto R^{-q}$ (Velikhov 1959, Chandrasekhar 1960). The instability that follows has been given many names: the Velikhov-Chandrasekhar, Balbus-Hawley, or magnetorotational instability. Balbus & Hawley (1991) were the first to realise its importance in accretion disks with Keplerian rotation profiles ($q = 3/2$). Flat galactic rotation curves are also unstable [MRIanim.gif].

Magnetorotational instability

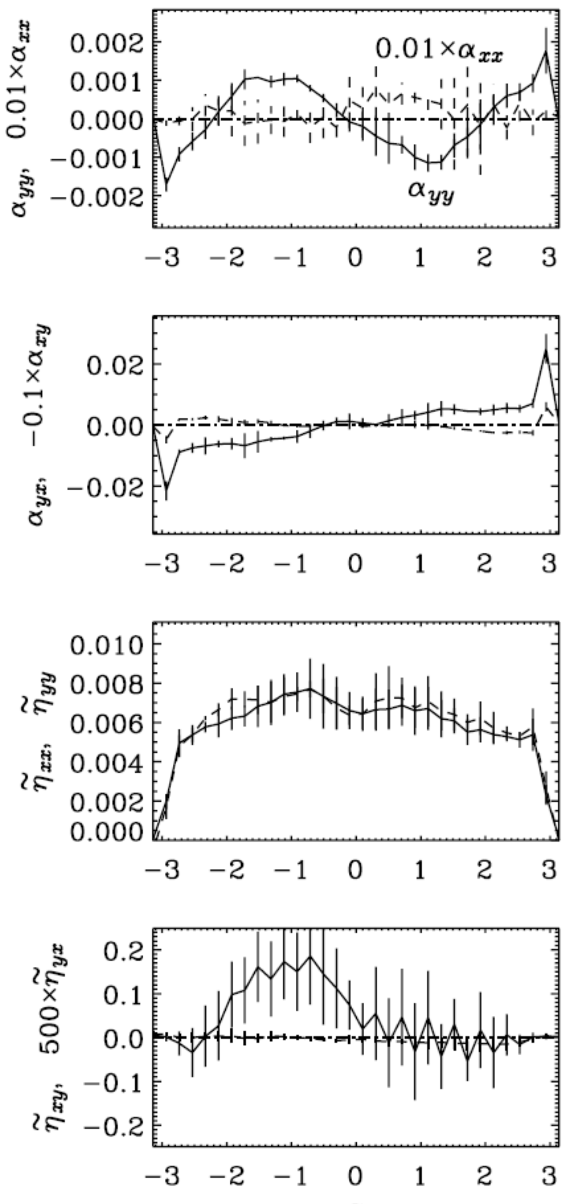

Unlike the thermal instability, the MRI generates self-sustained turbulence. MRI-active turbulent flow can also act as a dynamo, as in the case of accretion disks (e.g. Brandenburg et al. 1995). The properties of the turbulence and dynamo, however, are quite different from the SN-forced flow. The most striking properties of MRI-dynamo are the superequipartition magnetic fields (magnetic energy dominates over kinetic one) and the turbulent transport coefficients (notably the $\alpha_{\phi\phi}$ component of different sign). Figure is from Brandenburg (2005), where the turbulent transport coefficients were determined with the test field method.

Galactic MRI?

Flat galactic rotation laws are MRI-unstable, so shouldn't we expect to see some sort of SN-MRI-dynamo? SN-forced flow models (so far) have shown no signatures of MRI. Why? Korpi et al. (2010) discussed a possibility of MRI damping due to the very effective turbulent mixing, and therefore also enhanced turbulent Ohmic diffusion, due to SNe. Based on linear stability analysis of non-ideal MRI, FOSA, and taking into account some very basic properties of SN-forced flows, they estimated that MRI could be damped by SN activity up to the radius of roughly 14 kpc. Outside this radius, the most likely source of turbulence and also dynamo action is indeed MRI.